# ac conductivity in La2CuO4

**Peter Lunkenheimer, M. Resch, Alois Loidl, Y. Hidaka**

**Angaben zur Veröffentlichung / Publication details:**

Lunkenheimer, Peter, M. Resch, Alois Loidl, and Y. Hidaka. 1992. "ac conductivity in La2CuO4." *Physical Review Letters* 69 (3): 498–501. https://doi.org/10.1103/physrevlett.69.498.



# ac Conductivity in $La_2CuO_4$

P. Lunkenheimer, M. Resch, and A. Loidl
*Institut für Physik, Universität Mainz, 6500 Mainz, Germany*

Y. Hidaka
*NTT Interdisciplinary Research Laboratories, 162 Tokai, Ibaraki, 319-11, Japan*
(Received 23 December 1991)

Measurements of the complex ac conductivity are reported for a single crystal of $La_2CuO_4$ for frequencies $10^2 \leq \nu \leq 10^9$ Hz and temperatures $25 \leq T \leq 300$ K. The conductivity follows a power-law behavior $\omega^s$ with the frequency exponent $s$ independent of temperature and independent of frequency. However, the hopping transport is strongly anisotropic, with $s \approx 0.75$ within the $CuO_2$ planes and $s \approx 0.25$ perpendicular to the planes.

PACS numbers: 72.20.Fr, 72.80.Jc, 74.70.Vy

The discovery of superconductivity in $La_{2-x}Ba_xCuO_{4+\delta}$ by Bednorz and Müller [1] and the observation of even higher transition temperatures in related cuprates have led to intensive studies of the electrical transport properties of the metallic ($x \approx 0.2$, $\delta \approx 0$) and the semiconducting "parent" compounds ($x \approx 0$, $\delta \approx 0$). Strong electron correlations within the $CuO_2$ planes give rise to antiferromagnetism [2] and to the insulating properties [3] of the undoped materials. Doping with holes ($x > 0$ [4], $\delta > 0$ [5]) drives the insulator-to-metal transition (IMT) and destroys long-range magnetic order. The occurrence of superconductivity in close vicinity to an IMT supported speculations that the superconductivity could be due to a condensation of bipolarons [6]. And indeed, experimental evidence for polaron hopping has been reported in a large number of superconducting cuprates [7] and in semiconducting $Bi_4Sr_3Ca_3Cu_4O_x$ [8] (which becomes superconducting when properly annealed). In $La_2CuO_4$ evidence for extremely heavy charge carriers and a high dielectric constant has been reported from millimeter-wave conductivity measurements [9]. However, these results are at odds with results of ac conductivity measurements at audio frequencies in $La_2CuO_4$ [10] and $YBa_2Cu_3O_6$ [11]. In these compounds Chen *et al.* [10] and Samara *et al.* [11] detected hopping conductivity characteristic of doped semiconductors.

In this Letter we report measurements of the ac conductivity in single crystals of $La_2CuO_4$ in a frequency range from $10^2 \leq \nu \leq 10^9$ Hz and for temperatures $10 \leq T \leq 300$ K. The results provide clear evidence that the hopping conduction is extremely anisotropic.

Single crystals were grown from CuO flux and subsequently tempered for 50 h at 800 °C in oxygen flow. Details concerning the crystal growth are given in Ref. [12]. No traces of superconductivity were found, either in conductivity experiments, or in dc-magnetization measurements using a SQUID magnetometer (Meissner measurements) [13]. Magnetic susceptibility anomalies occurred close to 150 K and were interpreted to signal the onset of antiferromagnetic long-range order [13]. Depending on the oxygen content $\delta$, antiferromagnetism was reported to occur in $La_2CuO_{4+\delta}$ in a temperature range $50 < T_N < 250$ K [14]. Superconductivity in $La_2CuO_4$ is attributed to the presence of excess oxygen ($\delta > 0$) [5]. From the bulk measurements we conclude that $\delta$ in our sample is smaller than 0.02, although $T_N$ is significantly lower than the values reported in Ref. [5], as determined from powder samples.

At high frequencies, $10^6 \leq \nu \leq 10^9$ Hz, the complex conductivity, $\sigma = \sigma' + i\sigma''$, has been recorded using a HP 4191A impedance analyzer connected to a refrigerator system (CTI Cryogenics) via an air line [15]. At audio frequencies ($10^2 \leq \nu \leq 10^6$ Hz) automated low-frequency bridges have been used. The measurements were performed along all three crystallographic directions of a crystal with $3 \times 2 \times 1.3$ mm$^3$. Hence, the field was oriented within the $CuO_2$ planes (**E**$\|$**a** and **E**$\|$**b**) or perpendicular to them (**E**$\|$**c**). As a result of the twinning of the crystal it is not possible to distinguish the two directions within the plane as verified experimentally. Reflectometric methods require two-point contact configurations. Thus, to make electrical contacts the two surfaces normal to the field direction were covered with silver paint. Such contacts have a large resistance at low frequencies ($\nu < 10^6$ Hz). In the data analysis we made a special effort to take the influence of the contacts into account. In addition, the "dc resistivity" ($\nu = 113$ Hz) has been measured using a standard four-probe technique and lock-in amplifiers.

Figure 1 shows the temperature dependence of the resistivity from the four-probe measurements within the $CuO_2$ planes. It is well documented in the literature [16] that the strong increase of the resistivity with decreasing temperature can be well described by the Mott variable-range-hopping (VRH) model [17]. In this model it is assumed that the charge carriers move along a path determined by the optimal pair hopping rate from one localized state to another. Band conduction is absent because the extended states are too far away from the Fermi level. We fitted the data with the standard Mott equations $\rho = \rho_0 \exp[(T_0/T)^\gamma]$ with the exponent $\gamma = 1/4$ for three-dimensional and the exponent $\gamma = 1/3$ for two-dimen-

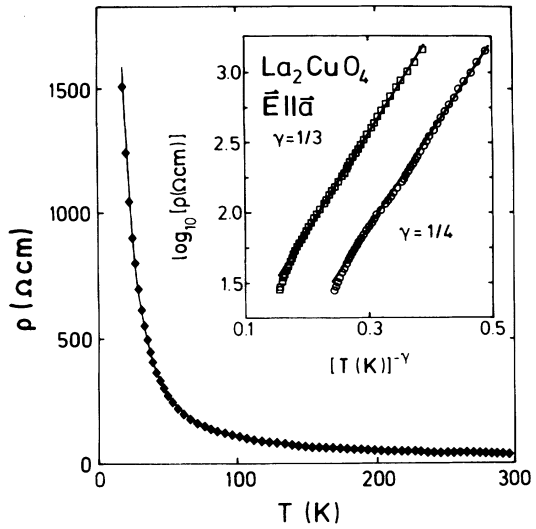


FIG. 1. dc resistivity (113 Hz) in $La_2CuO_4$ vs temperature with the field directed within the $CuO_2$ planes. The inset shows a representation of the experimental results as $\log_{10}(\rho)$ vs $T^{-\gamma}$, with $\gamma=1/3$ and 1/4. The solid lines represent fits as described in the text.

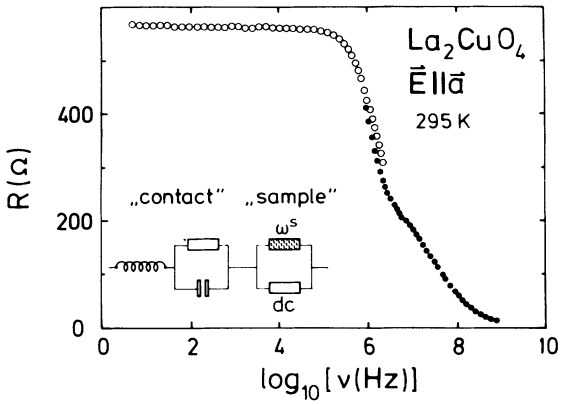


FIG. 2. Room-temperature ac impedance in $La_2CuO_4$ vs the logarithm of the measuring frequency with the field directed within the $CuO_2$ planes. The network which has been used in the fits is indicated. The experimental data indicated by open and solid circles were measured using two different experimental techniques.

sional hopping. In addition we fitted the data with the form $\rho=\rho_0(T/T_0)^{1/2}\exp[(T_0/T)^{1/4}]$ [16]. Here the square-root prefactor takes into account correlation effects between the charge carriers. The least-squares fitting of the latter model is shown as a solid line in Fig. 1. The best fit yielded $\rho_0=5.5$ Ω cm, $T_0=2\times10^6$ K, and $\chi^2=2.84$ where $\chi^2$ is the weighted sum of the squared deviations. The values of $\rho_0$ and $T_0$ are in rough agreement with those reported by Kastner *et al.* [16] for crystals grown from CuO flow. Fitting with the standard VRH model yielded $\rho_0=2.93$ Ω cm, $T_0=4.65\times10^3$ K, and $\chi^2=2.56$ for $\gamma=1/3$ and $\rho_0=0.76$ Ω cm, $T_0=6.07\times10^5$ K, and $\chi^2=4.56$ for $\gamma=1/4$. The best fits with the standard VRH model are shown in the inset of Fig. 1. Here we used the representation $\log_{10}(\rho)$ vs $T^{-\gamma}$ to account for the different exponents in the models for the two- and three-dimensional hopping. Assuming a plausible density of states, which can be determined from measurements of the Pauli spin susceptibility, the localization lengths are of the order of approximately 1 nm. A more detailed discussion of the dc-VRH results will be given in a forthcoming paper. Although the quality of the fits slightly favors two-dimensional hopping, we do not want to overemphasize the significance of these results. Two-dimensional variable-range hopping in $La_{2-x}Sr_xCuO_4$ has been reported by Aliev *et al.* [18] to occur at low temperatures.

Figure 2 shows the room-temperature raw data of the low-frequency (open circles) and the high-frequency resistance (solid circles) measured with two experimental setups. The field was directed within the $CuO_2$ planes (E||a). For low frequencies, $\nu<10^6$ Hz, the resistance is solely determined by the contacts which act like a leaky capacitor. The power-law behavior of the hopping conductivity of the sample significantly contributes to the high-frequency impedance ($\nu>10^6$ Hz) only.

Figure 3 shows the logarithm of the real and imaginary parts of the conductivity versus the logarithm of the measuring frequency ($\nu\geq10^6$ Hz) with E||a at different temperatures. At low temperatures and especially in the imaginary part of the conductivity a pure power-law behavior $\sigma''\sim\omega^s$ (the angular frequency $\omega=2\pi\nu$), i.e., with an exponent $s$ independent of frequency, is observed. At higher temperatures and frequencies $\nu<10^8$ Hz the contacts contribute significantly to the ac response. We have taken these observations into account by fitting the data using the network indicated in Fig. 2. Here the leaky capacitor represents the contacts. For the sample conductivity we assumed a pure power-law behavior with the same frequency exponent $s$ for $\sigma'$ and $\sigma''$ and a ratio $\sigma''/\sigma'=\tan(s\pi/2)$ which follows from the Kramers-Kronig relation for $s<1$ [19]: $\sigma'=\sigma_{dc}+\sigma_0\omega^s$; $\sigma''=\omega\times\varepsilon_0\varepsilon_\infty+\tan(s\pi/2)\sigma_0\omega^s$. $\sigma_{dc}$ is the dc conductivity of the sample, $\varepsilon_\infty$ the high-frequency dielectric constant, and $\varepsilon_0$ the permittivity of free space. The solid lines in Fig. 3 are the results of simultaneous fits to $\sigma'(\omega)$ and $\sigma''(\omega)$. The model involves six relevant parameters, namely, $\sigma_{dc}$, $\sigma_0$, and $s$ to describe the properties of the cuprate sample and $C$, $R_k$, and $L$ to model the behavior of the contacts. At radio frequencies significant contact contributions are observed at high temperatures only. At room temperature the fits yielded $\sigma_{dc}=2.0\times10^{-2}$ $(\Omega\,\text{cm})^{-1}$, $\sigma_0=1.3\times10^{-8}$ $(\Omega\,\text{cm})^{-1}$, $s=0.70$, $R_k=270$ Ω, $C=340$ pF, and $L=0.90$ nH. $\varepsilon_\infty$ is negligible. The agreement between experimental results and model predictions is almost perfect. The fits yielded an exponent $s$ of the order of 0.75, which is only weakly dependent on temperature (lower inset of Fig. 3). The intrinsic ac conductivity of the sam-

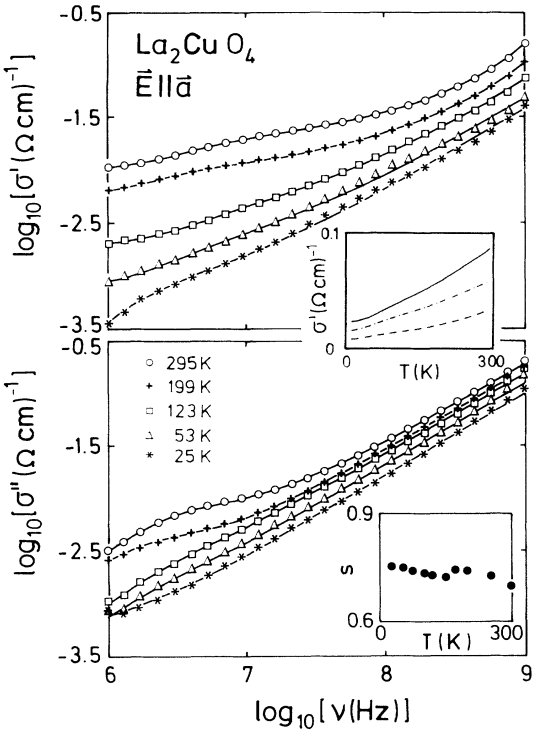


FIG. 3. Frequency dependence of the real (top) and imaginary (bottom) parts of the complex in-plane conductivity in $La_2CuO_4$, at various temperatures. The solid lines represent the results of fits using the network indicated in Fig. 2. The upper inset shows the temperature dependence of the real part of the ac conductivity for 110 MHz (dashed line), 331 MHz (dash-dotted line), and 575 MHz (solid line). The lower inset shows the temperature dependence of the frequency exponent $s$.

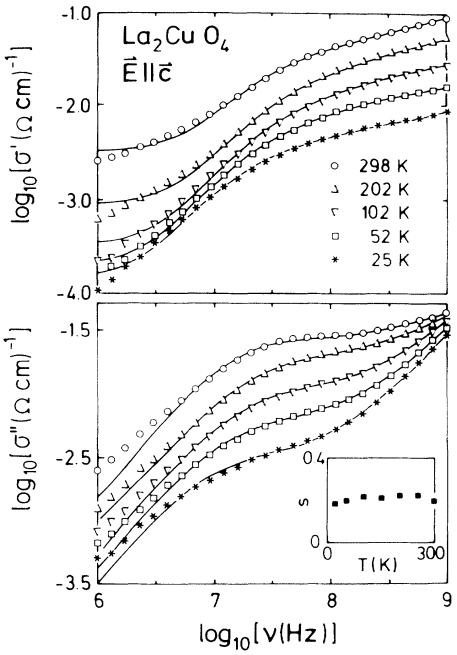


FIG. 4. Frequency dependence of the real (top) and imaginary (bottom) parts of the complex out-of-plane conductivity in $La_2CuO_4$, at various temperatures. The solid lines represent the results of fits using the network indicated in Fig. 2. The inset in the lower part of the figure shows the temperature dependence of the frequency exponent $s$.

ple reveals an almost linear temperature dependence. This is demonstrated in the upper inset of Fig. 3 for frequencies $\nu > 10^8$ Hz where the contact contributions can be neglected. Very similar results have been obtained for **E**||**b**.

The results for the conductivity with the field directed perpendicular to the $a$-$b$ plane are shown in Fig. 4. Obviously, the ac responses within and perpendicular to the $CuO_2$ planes look very different. For **E**||**c** the frequency exponent $s$ is hidden by a complex relaxation behavior. Nevertheless, the data can be fitted with the same network as indicated in Fig. 2. The parameters which describe the hopping conductivity along **c** [$s=0.2$ and $\sigma_0 = 8.1\times10^{-4}$ $(\Omega\,\mathrm{cm})^{-1}$] differ drastically from those observed for **E**||**a**. $C$, $R_k$, and $L$ are similar for both field directions. Again $s$ is frequency independent and only weakly dependent on temperature (see the inset of the lower frame in Fig. 4). Admittedly the quality of the fit is not as good as for the two in-plane directions and characteristic deviations occur at low frequencies. This provides experimental evidence that between the $CuO_2$ planes a rather different hopping mechanism must be considered.

ac conductivity data in $La_2CuO_{4+\delta}$ for frequencies up to $10^7$ Hz have been reported recently by Chen *et al.* [10] for different hole-doping levels $\delta$. Their main results were that $s$ strongly depends on $\delta$ and reaches values close to 0.8 at low temperatures and light doping. However, they reported a strong temperature dependence of the frequency exponent and an almost isotropic hopping behavior. Both results are in clear contradiction to our findings.

The dc results (Fig. 1) clearly favor an interpretation in terms of the VRH model which also makes definite predictions concerning the ac conductivity [20]: $\sigma_{ac}$ is predicted to increase linearly in $T$; real and imaginary parts reveal a complex frequency dependence, $\sigma' \sim \omega^{s'(\omega)}$, $\sigma'' \sim \omega^{s''(\omega)}$ with $s'' < s'$. Both frequency exponents are independent of temperature and decrease with increasing frequency. Our results reveal a linear temperature dependence of $\sigma_{ac}$ and a temperature-independent frequency exponent. However, our data document that $s' = s''$, both independent of frequency (low temperatures in Fig. 3), which is in disagreement with the VRH predictions.

So far we have no explanation for the large anisotropy of the exponent $s$, which indicates the presence of rather different hopping mechanisms for hops within and perpendicular to the $CuO_2$ planes. The deviations from the fits at low frequencies, as indicated in Fig. 4, point toward a more complex behavior of the charge transport along **c**. From a preliminary analysis we conclude that a pure re-

laxational motion of charge carriers is superimposed on the tunneling motion. This relaxation may well be due to contributions from bound polarons which reorient with a mean relaxation time of the order of $10^{-8}$ s. An alternative interpretation can be given by assuming a screening of the localized charge carriers by mobile carriers. As in typical charge density wave systems, a relaxation peak should occur at a frequency $\nu_p = 1/2\pi\rho\varepsilon$ [21]. With $\rho \approx 1000\ \Omega$ cm and $\varepsilon = 23\varepsilon_0$ [9] the result is $\nu_p = 8\times10^7$ Hz. It is interesting to note that in the charge-density-wave system $TaS_3$ a power-law frequency dependence of $\sigma$ with $s < 1$ has been observed also [22].

The value of the frequency exponent for in-plane hopping, as well as the findings of an only weak temperature dependence of $s$, bears the signature of tunneling of charge carriers between localized states and is a common feature of ac conductivities in disordered materials [20]. Further evidence for tunneling comes from the dc measurements and from the linear temperature dependence of $\sigma_{ac}$. Therefore we conclude that tunneling is the dominant charge-transport mechanism in $La_2CuO_4$. However, the facts that $s$ is frequency independent up to GHz frequencies, that $s'' = s'$, and that $s$ is strongly anisotropic cannot be explained in the framework of the VRH model.

This work was supported by the Sonderforschungsbereich 252 (Darmstadt/Frankfurt/Mainz/Stuttgart) and by the Bundesministerium für Forschung und Technologie under Contract No. 13N5705.

[1] J. G. Bednorz and K. A. Müller, Z. Phys. B **64**, 189 (1986).
[2] D. Vaknin *et al.*, Phys. Rev. Lett. **58**, 2802 (1987).
[3] J. D. Jorgensen *et al.*, Phys. Rev. Lett. **58**, 1024 (1987).
[4] A. Aharony *et al.*, Phys. Rev. Lett. **60**, 1330 (1988).
[5] B. Dabrowski *et al.*, Physica (Amsterdam) **162-164C**, 99 (1989).
[6] P. Prelovsek *et al.*, J. Phys. C **20**, L229 (1987); F. C. Zhang and T. M. Rice, Phys. Rev. B **37**, 3759 (1988); L. J. de Jongh, Physica (Amsterdam) **152C**, 171 (1988).
[7] D. Mihailovic *et al.*, Phys. Rev. B **42**, 7989 (1990).
[8] A. Gosh and B. K. Chaudhuri, Phys. Rev. B **41**, 1581 (1990); A. Gosh and D. Chakravorty, J. Phys. Condens. Matter **2**, 649 (1990).
[9] D. Reagor *et al.*, Phys. Rev. Lett. **62**, 2048 (1989).
[10] C. Y. Chen *et al.*, Phys. Rev. Lett. **63**, 2307 (1989).
[11] G. A. Samara *et al.*, Phys. Rev. B **41**, 8974 (1990).
[12] Y. Hidaka *et al.*, J. Cryst. Growth **85**, 581 (1987).
[13] M. Lang, Ph.D. thesis, Technische Hochschule Darmstadt, 1991 (unpublished).
[14] T. Freloft *et al.*, Phys. Rev. B **36**, 826 (1987).
[15] R. Böhmer *et al.*, J. Appl. Phys. **65**, 901 (1989).
[16] M. A. Kastner *et al.*, Phys. Rev. B **37**, 111 (1988); C. Uher and A. B. Kaiser, Phys. Rev. B **37**, 127 (1988).
[17] N. F. Mott, Philos. Mag. **19**, 835 (1969); Rev. Mod. Phys. **50**, 203 (1978); N. F. Mott and E. A. Davies, *Electronic Processes in Non-Crystalline Materials* (Oxford Univ. Press, Oxford, 1971).
[18] F. G. Aliev *et al.*, J. Magn. Magn. Mater. **90&91**, 641 (1990).
[19] See, e.g., H. W. Bode, *Network Analysis and Feedback Amplifier Design* (Van Nostrand, Princeton, NJ, 1945), p. 314.
[20] A. R. Long, Adv. Phys. **31**, 553 (1982); S. R. Elliott, Adv. Phys. **36**, 135 (1987).
[21] J. R. Tucker *et al.*, Phys. Rev. B **34**, 9038 (1986); P. B. Littlewood, Phys. Rev. B **36**, 3108 (1987).
[22] Wei-yu Wu *et al.*, Phys. Rev. Lett. **52**, 2382 (1984).